EXTENDED EXPERIMENTAL PROCEDURES

Preparation of Dendritic Cells

BMDCs were generated from 6- to 8-week-old female C57BL/6J mice (Jackson Laboratories). Bone marrow cells were collected from femora and tibiae and plated at 10^6 cells/ml on nontissue culture treated petri dishes in RPMI-1640 medium (GIBCO), supplemented with 10% FBS, L-glutamine, penicillin/streptomycin, MEM nonessential amino acids, HEPES, sodium pyruvate, β-mercaptoethanol, and murine GM-CSF (15 ng/ml; Peprotech) or human Flt3L (100 ng/ml; Peprotech). GM-CSF-derived BMDCs were used directly for all RNAi experiments. For all other experiments, floating cells from GM-CSF cultures were sorted at day 5 by MACS using the CD11c (N418) MicroBeads kit (Miltenyi Biotec). Sorted $CD11c^+$ cells were used as GM-CSF-derived BMDCs, and plated at 10^6 cells/ml and stimulated at 16 hr post sorting. For Flt3L culture, floating cells were harvested at days 6–8 and used as Flt3L-derived BMDCs by plating them at 10^6 cells/ml and stimulating 16 hr later.

For SILAC experiments, GM-CSF-derived BMDCs were grown in media containing either normal L-arginine (Arg0) and L-lysine (Lys0) (Sigma) or L-arginine 13C6-15N4 (Arg10) and L-lysine 13C6-15N2 (Lys8) (Sigma Isotec). Concentrations for L-arginine and L-lysine were 42 mg/l and 40 mg/l, respectively. The cell culture media, RPMI-1640 deficient in L-arginine and L-lysine, was a custom media preparation from Caisson Laboratories (North Logan, UT) and dialyzed serum was obtained from SAFC-Sigma. We followed all standard SILAC media preparation and labeling steps as previously described (Ong and Mann, 2006).

Preparation of Primary Lung Fibroblasts

MLFs were derived from lung tissue from 6- to 8-week-old female C57BL/6J mice (Jackson Laboratories). MLFs were isolated as previously described (Tager et al., 2004). Briefly, lungs were digested for 45 min at 37°C in collagenase and DNase I, filtered, washed, and cultured in DMEM supplemented with 15% FBS. Cells were used for experiments between passages 2 and 5.

Genetically Modified Mice

Bone marrow from *Plk2*$^{-/-}$ mice and their wild-type littermates were obtained from Elan Pharmaceuticals (Inglis et al., 2009). *Ifnar1*$^{-/-}$ mice on a C57BL/6J background were a gift from Kate Fitzgerald (originally from Jonathan Sprent based on Muller et al., 1994). Heterozygous *Crkl*$^{+/-}$ mice on a C57BL/6J background were obtained from the Jackson Laboratory. *Crkl*$^{+/-}$ C57BL/6J mice were crossed to wild-type Black Swiss mice from Taconic, as *Crkl*$^{-/-}$ mice on a pure C57BL/6J genetic background have been reported to be embryonic lethal (Guris et al., 2001; Hemmeryckx et al., 2002). Heterozygous *Crkl*$^{+/-}$ offspring were backcrossed to *Crkl*$^{+/-}$ C57BL/6J mice to obtain *Crkl*$^{-/-}$ mice. Mice were kept in a specific pathogen-free facility at MIT. Animal procedures were in accordance with National Institutes of Health Guidelines on animal care and use and were approved by the MIT Committee on Animal Care (Protocol #0609-058-12).

Viruses

SeV, strain Cantell, and EMCV, strain EMC, were from ATCC. NDV, strain Hitchner B1 was from Aldolfo Garcia-Sastre (Mount Sinai School of Medicine), and VSV, strain Indiana was from Ulrich von Andrian (Harvard Medical School). Influenza A virus strain A/PR/8/34 and ΔNS1 were grown in Vero cells (which allow efficient growth of the ΔNS1 virus) in serum-free DMEM supplemented with 10% BSA and 1 mg/ml TPCK trypsin. Viral titers were determined by standard MDCK plaque assay. To measure the amount of VSV RNA present in infected tissues, we used previously reported qPCR primers: VSV forward 5′-TGATACAGTACAATTATTTTGGGAC-3′, and VSV reverse 5′-GAGACTTTCTGTTACGGGATCTGG-3′ (Hole et al., 2006). Viruses were handled according to CDC and NIH guidelines with protocols approved by the Broad Institutional Biosafety Committee.

Reagents

TLR ligands were from Invivogen (Pam3CSK4, ultra-pure *E. coli* K12 LPS, ODN 1585 CpG type A, and ODN 1668 CpG type B) and Enzo Life Sciences (poly(I:C)), and were used at the following concentrations: Pam3CSK4 (250 ng/ml), poly(I:C) (10 μg/ml), LPS (100 ng/ml), CpG-A (10 μg/ml), CpG-B (10 μg/ml). Heat-killed *Listeria monocytogenes* (HKLM) was from Invivogen. Polo-like kinase inhibitors were from Selleck (BI 2536; Steegmaier et al., 2007), Sigma (GW843682X, also known as compound 1 and GSK461364; Lansing et al., 2007), and Chembridge (Poloxipan; Reindl et al., 2009). SP 600125 (Jnk inhibitor) was from Enzo Life Sciences. Image-iT FX Signal Enhancer, DAPI, and Alexa Fluor Labeled Secondary Antibodies were obtained from Invitrogen. For immunofluorescence, antibodies against IRF3 (4302S) and NF-κB P65 (4764S) were obtained from Cell Signaling Technology. For cell viability assays, Alamar Blue was from Invitrogen and CellTiter-Glo from Promega.

Virus Titering of MLF Supernatant

293T cells were seeded and transfected with a vRNA luciferase reporter plasmid as previously described (Shapira et al., 2009). Briefly, at 24 hr post-transfection, 10^4 transfected reporter cells were reseeded in white Costar plates. Supernatants from influenza-infected MLFs were added to reporter cells and incubated for 24 hr. Reporter activity was measured with firefly luciferase substrate (Steady-Glo, Promega). Luminescence activity was quantified with the Envision Multilabel Reader (Perkin Elmer).

Cell-Cycle Analysis

Cells were fixed in ethanol, washed, and stained for 30 min at room temperature (RT) with propidium iodide (100 μg/ml) prepared in PBS (calcium- and magnesium-free) supplemented with RNase A (2 mg/ml; Novagen) and Triton X-100 (0.1%). Samples were analyzed for DNA content using an Accuri C6 flow cytometer (Accuri) and data was processed using the FlowJo software (Treestar).

ELISA

Cell culture supernatants were assayed using a sandwich ELISA kit for mouse IFN-β (PBL Biomedical Laboratories).

mRNA Isolation

Total RNA was extracted with QIAzol reagent following the miRNeasy kit's procedure (QIAGEN), and sample quality was tested on a 2100 Bioanalyzer (Agilent). RNA was reverse transcribed with the High Capacity cDNA Reverse Transcription kit (Applied Biosystems). For experiments with more than 12 samples, we harvested Poly(A)$^+$ RNA in 96- or 384-well plates with the Turbocapture mRNA kit (QIAGEN) and reverse transcribed with the Sensiscript RT kit (QIAGEN).

qPCR Measurements

Real-time quantitative PCR reactions were performed on the LightCycler 480 system (Roche) with FastStart Universal SYBR Green Master Mix (Roche). Every reaction was run in triplicate and GAPDH levels were used as an endogenous control for normalization.

shRNA Knockdowns

High-titer lentiviruses encoding shRNAs targeting genes of interest were obtained from The RNAi Consortium (TRC; Broad Institute, Cambridge, MA, USA) (Moffat et al., 2006). Bone marrow cells were infected with lentiviruses as described (Amit et al., 2009). For each gene of interest, we tested five shRNAs for knockdown efficiency using qPCR of the target gene. We selected shRNAs with >75% knockdown efficacy. For combinatorial knockdown, two independent mixtures of two lentiviruses encoding validated shRNAs against *Plk2* and *4*, respectively, were used to infect bone marrow cells (two *Plk2*- and two *Plk4*-specific shRNAs were used to generate these mixtures). Lentivirus-infected cells were composed of ~90% CD11c$^+$ cells, which was comparable to sorted BMDCs and to our previous observations (Amit et al., 2009).

mRNA Measurements on nCounter

Details on the nCounter system are presented in full in (Geiss et al., 2008). We used a custom CodeSet constructed to detect a total of 128 genes (including 10 control genes whose expression remain unaffected by TLR stimulation) selected by the GeneSelector algorithm (Amit et al., 2009) as described below. 5×10^4 BMDCs were lysed in RLT buffer (QIAGEN) supplemented with 1% β-mercaptoethanol. Ten percent of the lysate was hybridized for 16 hr with the CodeSet and loaded into the nCounter prep station followed by quantification using the nCounter Digital Analyzer following the manufacturer's instructions.

Custom Nanostring CodeSet Construction using the GeneSelector Algorithm

We used the CodeSet that we previously used and described in Amit et al., 2009. Briefly, to choose a set of genes that will capture as much as possible of the information on the expression of all genes, we used an information-theoretic approach. We modeled the expression levels X given the experimental condition C with a naive Bayes model where the expression of gene i under condition c follows a normal distribution $X_i|C=c \sim N(\mu_{ic}, \sigma_i^2)$. In this model, the expression levels of all genes depend on the experimental condition C, and we selected genes that are highly informative about C. Formally, for a set of genes Y we used the conditional entropy $H(C|\mathbf{Y}) = -\sum_c p(C=c)\sum_y p(Y=y|C=c)\log p(C=c|Y=y)$ as a measure of the remaining uncertainty in C once the expression levels Y are known. We then used this measure and a greedy procedure to select multiple disjoint gene sets, $Y_1, \ldots, Y_k$ such that for each set Y_i, $H(C|Y_i)<\eta$ (we set $\eta = 0.5$). In the greedy procedure, we select genes one at a time, and with each selected gene recompute the entropy given the genes already selected in the current set. Once a set is complete (the remaining conditional entropy is below the threshold η), we add all the genes to the selected set, and repeat the procedure (excluding all the selected genes from consideration). We stop when the number of selected genes has reached a user-defined threshold, set by the number of genes feasible for the experimental assay.

To select a time point, we used the same approach. Here, we measured entropy under all time points for multiple randomly selected gene sets of several sizes and plotted the average entropy for each time point (see Amit et al., 2009). We chose the time point with the minimal entropy (i.e., 6 hr post-simulation).

nCounter Data Analysis

After normalization by internal Nanostring controls (spike-normalization following manufacturer's instructions), we normalized the data relying on three control genes (*Ndufa7*, *Tbca*, *Tomm7*) that are the least affected by shRNAs and LPS stimulation. Next, we log-transformed the expression values (Bengtsson and Hossjer, 2006). Five signature genes (*Cxcl5*, *Fos*, *Fst*, *Ereg*, and *Egr2*) that were highly variable across control shRNA samples were removed from subsequent analysis. To score target genes whose expression is significantly affected by perturbations, we used a fold threshold corresponding to an FDR of 2%. For a given shRNA perturbation, a target gene was called as significantly affected when the ratio of the log-expression of this gene upon shRNA knockdown to

the average log-expression of this gene in control shRNA samples was below (or above) a threshold (1/threshold), chosen such that, on average, no more than 2 hits (out of 128 genes in the Nanostring codeset) per control shRNA sample were called. Heatmaps and distance matrix analyses were generated using the software Gene-E (http://www.broadinstitute.org/cancer/software/GENE-E/).

Microarray Hybridization and Processing

For oligonucleotide microarray hybridization, 1 μg of RNA were labeled, fragmented, and hybridized to an Affymetrix Mouse Genome 430A 2.0 Array. After scanning, the expression value for each gene was calculated with RMA (Robust Multi-Array) normalization. The average intensity difference values were normalized across the sample set. Probe sets that were absent in all samples according to Affymetrix flags were removed. All values below 50 were floored to 50.

Detection of Regulated Signaling Genes

To identify differentially regulated signaling components (i.e., kinases, phosphatases, and signaling adaptors or scaffolds), we defined regulated probesets for each condition (TLR agonist) as probesets displaying at least 1.7-fold up- or downregulation in both duplicates of at least one time point, compared to unstimulated controls, using our previously published microarray dataset available in the NCBI Gene Expression Omnibus under the accession number GSE17721 (Amit et al., 2009). Differentially regulated probesets were intersected with lists of kinases, phosphatases, and signaling adaptors and scaffolds. These gene sets were generated combining data from publicly available databases: Panther (http://www.pantherdb.org), Gene Ontology (http://www.geneontology.org), and DAVID (http://david.abcc.ncifcrf.gov). Regulated signaling genes were hierarchically clustered using the Cluster software (Eisen et al., 1998).

Antiviral versus Inflammatory Gene Enrichment

Genes whose expression changed upon BI 2536 treatment in microarrays (Table S4) were evaluated for their enrichment with genes involved in the antiviral and inflammatory programs. When multiple probesets were available for a given gene on the microarray, only the probeset with maximum value was kept for analysis. Thus, the complete microarray consisted of 14,088 genes, among which 804 and 550 genes were identified as part of antiviral and inflammatory programs, respectively (Amit et al., 2009). We performed a hypergeometric test on genes whose expression changed at least 3-fold upon BI 2536 treatment compared to vehicle control (DMSO), in either LPS or poly(I:C) samples. In addition, genes whose expression changed upon BI 2536 treatment in microarrays in response to LPS and/or poly(I:C) stimulation were analyzed for enrichment of Gene Ontology (GO) processes and canonical pathways from curated databases using the Molecular Signature Databse (MSigDB; http://www.broadinstitute.org/gsea/msigdb/index.jsp).

Nanowire-Mediated Drug Delivery and Microscopy

BMDCs were plated on top of etched silicon nanowires (Si NWs) coated with small molecules (Shalek et al., 2010). After 24 hr, cells were stimulated with LPS or poly(I:C), then fixed in 4% formaldehyde in PBS (RT, 10 min). After fixation, each sample was permeabilized with 0.25% Triton X-100 in PBS (RT, 10 min), incubated with Image-iT FX Signal Enhancer (RT, 30 min), and then blocked with 10% goat serum and 0.25% Triton X-100 in PBS (RT, 1 hr). After washing, the samples were placed in 3% IgG-Free BSA & 0.25% Triton X-100 in PBS that contained primary antibodies against either IRF3 or NF-κB P65 (1:175 dilution) and then rocked overnight at 4°C. The following day, the samples were washed with PBS and then incubated with an Alexa Fluor labeled secondary antibody (1:250 dilution) in 3% IgG-Free BSA & 0.25% Triton X-100 in PBS (RT, 60 min). After washing with PBS, the samples were counterstained with 300 ng/ml of DAPI in PBS (RT, 30 min). For each experiment, every stimulus-molecule combination was prepared in triplicate. Once fixed, samples were imaged using an upright confocal microscope (Olympus). For each captured image, the nuclear fraction of the fluorescent protein was calculated after identifying nuclear boundaries using DAPI. Finally, distributions for this quantity across different conditions were compared using a one-way ANOVA analysis.

In Vivo BI 2536 Experiments in a VSV Infection Model

Eight-week-old C57BL/6 male mice (from Charles River Laboratories) received 500 μg of BI 2536 (or vehicle) intravenously, and 50 μg into the footpad 3 hr before and 2 hr after infection with 10^6 pfu of VSV, as previously described (Iannacone et al., 2010), into the footpad. Mice were sacrificed 6 hr post-infection and the draining popliteal lymph nodes were harvested in RNAlater solution (Ambion) before subsequent RNA analysis. All experimental animal procedures were approved by the Institutional Animal Committees of Harvard Medical School and IDI. All infectious work was performed in designated $BL2^+$ workspaces, in accordance with institutional guidelines, and approved by the Harvard Committee on Microbiological Safety.

Microwestern Arrays

The MWA method previously described (Ciaccio et al., 2010) was modified to accommodate a larger number of lysates. The lysates were printed in a ''double-block'' format with each MWA being 18 mm wide by 9 mm long. Twelve samples plus protein marker (Li-Cor 928-40000) were printed with a noncontact piezoelectric arrayer (GeSiM NP2) along the top edge of the block, each block printed forty-eight times on the acrylamide gel. The deck layout is included in Figure S7A. Electrophoresis, transfer, and antibody incubation were performed as previously described with the exception of using a modified 48-well gasket (The Gel Company MMH96) manually cut to have a larger block size in order to isolate antibodies on the nitrocellulose membrane per printed block. The antibodies used in

this study were against β-ACTIN, GAPDH, β-TUBULIN, IκBα (clone L35A5), P65 (clone C22B4), STAT1, p-ABL(C-) (Y245), p-AKT (S473), p-AKT1/2/3 (T308), p-ATF2 (T71), p-ERK1/2 (T202/Y204), p-IKBALPHA (S32), p-IKKA/B (S176/180), p-IRF3 (S396), p-MAPKAPK2 (T222), p-MEK(1/2) (S217/221), p-MET (Y1234/1235), p-P38 (T180/Y182), p-P65 (S536), p-P70S6K (S371), p-P70S6K (T389), p-P90RSK (S380), p-PI3K P85(Y458) P55(Y199), p-PKCD (Y311), p-SAPK/JNK (T183/Y185), p-SEK1/MKK4 (T261), p-STAT1 (S727), p-STAT1 (Y701), p-STAT3 (S727). All antibodies were from Cell Signaling Technology, except for β-ACTIN which was from Santa Cruz Biotechnology. Band intensities were quantified using Li-Cor Odyssey analysis software (V3.0). Circles were applied to the appropriate band on the scanned image and the net intensity was calculated by subtracting the background intensity from the trimmed mean intensity of each band. The net intensity was divided by the average net intensities of β-actin to control for lysate protein concentration. Fold Change was then calculated in relation to time of inhibitor application (time zero).

Phosphotyrosine Peptide Analysis

Tyrosine-phosphorylated peptides were prepared using a PhosphoScan Kit (Cell Signaling Technology) as previously described (Rush et al., 2005). Briefly, 100 million cells were lysed in lysis buffer (20 mM HEPES, 25 mM sodium pyrophosphate, 10 mM beta-glycerophosphate, 9 M urea, 1 mM ortho-vanadate, 1 Roche Ser/Thr phosphatase inhibitor tablet) assisted by sonication on ice using Misonix S-4000 sonicator with five 30 s bursts at 4 W. Lysates were precleared by centrifugation for 15 min at 20,000 g. Approximately 10 mg of total proteins from each SILAC label were mixed, reduced with 10 mM dithiothreitol and alkylated with 25 mM iodoacetamide. After 4-fold dilution 200 μg sequencing grade modified trypsin (Promega, V5113) was added in an enzyme to substrate ratio of 1:100. The total peptide mixtures were then desalted using a tC18 SepPak cartridge (Waters, 500 mg, W AT036790) and resuspended in IAP buffer (50 mM MOPS/NaOH [pH 7.2], 10 mM Na2HPO4, 50 mM NaCl). Peptide immunoprecipitation was performed with protein-G agarose bead-bound anti-phosphotyrosine antibodies pY100. Peptides captured by phosphotyrosine antibodies were eluted under acidic conditions (0.15% trifluoroacetic acid). The IP eluate was analyzed by data-dependent LC-MS/MS using a Thermo LTQ-Orbitrap instrument.

Global Serine, Threonine, and Tyrosine Phosphorylation Analysis

Quantitative analysis of serine-, threonine-, and tyrosine-phosphorylated peptides was performed essentially as described (Villén and Gygi, 2008) with some modifications. After stimulation, cells were lysed for 20 min in ice-cold lysis buffer (8 M Urea, 75 mM NaCl, 50 mM Tris [pH 8.0], 1 mM EDTA, 2 μg/ml Aprotinin (Sigma, A6103), 10 μg/ml Leupeptin (Roche, #11017101001), 1 mM PMSF, 10 mM NaF, 2 mM Na3VO4, 50 ng/ml Calyculin A (Calbiochem, #208851), Phosphatase inhibitor cocktail 1 (1/100, Sigma, P2850) and Phosphatase inhibitor cocktail 2 (1/100, Sigma, P5726). Lysates were precleared by centrifugation at 16,500 g for 10 min and protein concentrations were determined by BCA assay (Pierce). We obtained 3 mg total protein per label out of 30 million cells. Cell lysates were mixed in equal amounts per label and proteins were reduced with 5 mM dithiothreitol and alkylated with 10 mM iodoacetamide. Samples were diluted 1:4 with HPLC water (Baker) and sequencing-grade modified trypsin (Promega, V5113) was added in an enzyme to substrate ratio of 1:150. After 16 hr digest, samples were acidified with 0.5% trifluoroacetic acid (final concentration). Tryptic peptides were desalted on reverse phase tC18 SepPak columns (Waters, 500 mg, WAT036790) and lyophilized to dryness. Peptides were reconstituted in 500 μl strong cation exchange buffer A (7 mM KH_2PO_4, pH 2.65, 30% MeCN) and separated on a Polysulfethyl A column from PolyLC (250 × 9.4 mm, 5 μm particle size, 200 A pore size) using an Akta Purifier 10 system (GE Healthcare). We used an 80 min gradient with a 20 min equilibration phase with buffer A, a linear increase to 30% buffer B (7 mM KH2PO4, pH 2.65, 350 mM KCL, 30% MeCN) within 33 min, 100% B for 7 min and a final equilibration with Buffer A for 20 min. The flow rate was 3 ml/min and the sample was injected after the initial 20 min equilibration phase. Upon injection, 3 ml fractions were collected with a P950 fraction collector throughout the run. 60 fractions were collected of which 3–4 adjacent fractions were combined to obtain 12 samples. Pooling of SCX fractions was guided by the UV214-trace and fractions were combined starting where the first peptide peak appeared. The 12 samples were desalted with reverse phase tC18 SepPak columns (Waters, 100 mg, WAT036820) and lyophilized to dryness. SCX-separated peptides were subjected to IMAC (immobilized metal affinity chromatography) as described (Villén and Gygi, 2008). Briefly, peptides were reconstituted in 200 μl IMAC binding buffer (40% MeCN, 0.1% FA) and incubated for 1 hr with 5 μl of packed Phos-Select beads (Sigma, P9740) in batch mode. After incubation, samples were loaded on C18 StageTips (Rappsilber et al., 2007), washed twice with 50 μl IMAC binding buffer, and washed once with 50 μl 1% formic acid. Phosphorylated peptides were eluted from the Phos-Select resin to the C18 material by loading 3 times 70 μl of 500 mM K_2HPO_4 (pH 7.0). StageTips were washed with 50 μl of 1% formic acid to remove phosphate salts and eluted with 80 μl of 50% MeCN/0.1% formic acid. Samples were dried down by vacuum centrifugation and reconstituted in 8 μl 3% MeCN/0.1% formic acid.

NanoLC-MS/MS Analysis

All peptide samples were separated on an online nanoflow HPLC system (Agilent 1200) and analyzed on a LTQ Orbitrap Velos (Thermo Fisher Scientific) mass spectrometer. Four microliters of peptide sample were autosampled onto a 14 cm reverse phase fused-silica capillary column (New Objective, PicoFrit PF360-75-10-N-5 with 10 μm tip opening and 75 μm inner diameter) packed in-house with 3 μm ReproSil-Pur C18-AQ media (Dr. Maisch GmbH). The HPLC setup was connected via a custom-made electrospray ion source to the mass spectrometer. After sample injection, peptides were separated at an analytical flowrate of 200 nl/min with an 70 min linear gradient (~0.29%B/min) from 10% solvent A (0.1% formic acid in water) to 30% solvent B (0.1% formic

acid/90% acetonitrile). The run time was 130 min for a single sample, including sample loading and column reconditioning. Data-dependent acquisition was performed using the Xcalibur 2.1 software in positive ion mode. The instrument was recalibrated in real-time by coinjection of an internal standard from ambient air ("lock mass option") (Olsen et al., 2005). Survey spectra were acquired in the orbitrap with a resolution of 60,000 and a mass range from 350 to 1750 m/z. In parallel, up to 16 of the most intense ions per cycle were isolated, fragmented and analyzed in the LTQ part of the instrument. Ions selected for MS/MS were dynamically excluded for 20 s after fragmentation. For the second biological replicate analysis peptides observed to be regulated in the first analysis were loaded into a global parent mass inclusion list and 4 MS/MS scans were reserved for precursors from the inclusion list whereas 12 were performed on the most intense ions per duty cycle.

Identification and Quantification of Peptides and Proteins

Mass spectra were processed using the Spectrum Mill software package (Agilent Technologies) v4.0 b that includes in-house developed features for SILAC-based quantitation and phoshosite localization and also with the MaxQuant software package (version 1.0.13.13) (Cox and Mann, 2008), which was used in combination with a Mascot search engine (version 2.2.0, Matrix Science). For peptide identification in Spectrum Mill an International Protein Index protein sequence database (IPI version 3.60, mouse) was used which was reversed on-the-fly at search time. In MaxQuant a concatenated forward and reversed IPI protein sequence database (version 3.60, mouse) was queried. The mass tolerance for precursor ions and for fragment ions was set to 7 ppm and 0.5 Da, respectively. Cysteine carbamidomethylation was searched as a fixed modification, whereas oxidation on methionine, N-acetylation (Protein) and phosphorylation on serine, threonine, or tyrosine residues were considered as variable modifications. The enzyme specificity was set to trypsin and cleavage N-terminal of proline was allowed. The maximum of missed cleavages was set to 3. For peptide identification the maximum peptide FDR was set to 1%. The minimum identification score was to 5 in Spectrum Mill and to 10 in MaxQuant. SILAC ratios were obtained from the peptide export table in Spectrum Mill and the evidence table in MaxQuant. Arginine to Proline conversion was determined to be 3.42% and 5.55% for both biological replicates, respectively. The conversion was calculated by defining Arg-10 as a fixed modification and by quantifying the ratio between peptides containing normal L-proline (Pro0) and 13C5-15N1-labeled proline (Pro6) with MaxQuant. Each peptide SILAC ratio was corrected for arginine to proline conversion by the formula r[c] = r[o]/((1-p)^n), where r[c] is the corrected ratio, r[o] the observed ratio, p the conversion rate and n the number of proline residues per peptide. The median ratios of all nonphosphorylated peptides were used to normalize the M/L and H/L ratios of all phosphorylated peptides. To allow better peptide grouping, phosphosite localization information obtained from SpectrumMill and MaxQuant were further simplified. Probability scores greater or equal 0.75 were called fully localized and designated with (1.0), scores smaller 0.75 and greater or equal to 0.5 were called ambiguously localized and designated with (0.5), whereas scores smaller than 0.5 were called non-localized and the total number of phosphorylation sites per peptide was designated with an underscore after the peptide sequence. Median SILAC ratios of phosphopeptides for each experiment were calculated over all versions of the same peptide including different charge states and methionine oxidation states. The highest scoring versions of each distinct peptide were reported per experiment. Overlapping data between SpectrumMill and MaxQuant as well as between different biological replicates was analyzed for discrepancies by calculating the mean and standard deviation over all residuals for different ratios of the same phosphopeptide. Residuals were calculated by subtracting the two values for each phosphopeptide derived by SpectrumMill or MaxQuant as well as by two different biological replicates. All peptides were filtered from the data set that had residuals greater than 3 standard deviations distant from the mean as they were not reproducible between two biological replicates or between SpectrumMill and MaxQuant. Data derived from both software packages was combined and MaxQuant data was reported when the same phosphopeptide was identified and quantified by both programs. Log_2 phosphopeptide ratios of BI 2536 treated versus untreated dendritic cells followed a normal distribution that was fitted using least-squares regression. Mean and standard deviation values derived from the Gaussian fit were used to calculate p values. An FDR-based measure was used to assess significance of the findings (Storey and Tibshirani, 2003).

SUPPLEMENTAL REFERENCES

Amit, I., Garber, M., Chevrier, N., Leite, A.P., Donner, Y., Eisenhaure, T., Guttman, M., Grenier, J.K., Li, W., Zuk, O., et al. (2009). Unbiased reconstruction of a mammalian transcriptional network mediating pathogen responses. Science *326*, 257–263.

Bengtsson, H., and Hössjer, O. (2006). Methodological study of affine transformations of gene expression data with proposed robust non-parametric multi-dimensional normalization method. BMC Bioinformatics *7*, 100.

Ciaccio, M.F., Wagner, J.P., Chuu, C.P., Lauffenburger, D.A., and Jones, R.B. (2010). Systems analysis of EGF receptor signaling dynamics with microwestern arrays. Nat. Methods *7*, 148–155.

Cox, J., and Mann, M. (2008). MaxQuant enables high peptide identification rates, individualized p.p.b.-range mass accuracies and proteome-wide protein quantification. Nat. Biotechnol. *26*, 1367–1372.

Eisen, M.B., Spellman, P.T., Brown, P.O., and Botstein, D. (1998). Cluster analysis and display of genome-wide expression patterns. Proc. Natl. Acad. Sci. USA *95*, 14863–14868.

Geiss, G.K., Bumgarner, R.E., Birditt, B., Dahl, T., Dowidar, N., Dunaway, D.L., Fell, H.P., Ferree, S., George, R.D., Grogan, T., et al. (2008). Direct multiplexed measurement of gene expression with color-coded probe pairs. Nat. Biotechnol. *26*, 317–325.

Guris, D.L., Fantes, J., Tara, D., Druker, B.J., and Imamoto, A. (2001). Mice lacking the homologue of the human 22q11.2 gene CRKL phenocopy neurocristopathies of DiGeorge syndrome. Nat. Genet. *27*, 293–298.

Hemmeryckx, B., Reichert, A., Watanabe, M., Kaartinen, V., de Jong, R., Pattengale, P.K., Groffen, J., and Heisterkamp, N. (2002). BCR/ABL P190 transgenic mice develop leukemia in the absence of Crkl. Oncogene *21*, 3225–3231.

Hole, K., Clavijo, A., and Pineda, L.A. (2006). Detection and serotype-specific differentiation of vesicular stomatitis virus using a multiplex, real-time, reverse transcription-polymerase chain reaction assay. J. Vet. Diagn. Invest. *18*, 139–146.

Iannacone, M., Moseman, E.A., Tonti, E., Bosurgi, L., Junt, T., Henrickson, S.E., Whelan, S.P., Guidotti, L.G., and von Andrian, U.H. (2010). Subcapsular sinus macrophages prevent CNS invasion on peripheral infection with a neurotropic virus. Nature *465*, 1079–1083.

Inglis, K.J., Chereau, D., Brigham, E.F., Chiou, S.S., Schöbel, S., Frigon, N.L., Yu, M., Caccavello, R.J., Nelson, S., Motter, R., et al. (2009). Polo-like kinase 2 (PLK2) phosphorylates alpha-synuclein at serine 129 in central nervous system. J. Biol. Chem. *284*, 2598–2602.

Lansing, T.J., McConnell, R.T., Duckett, D.R., Spehar, G.M., Knick, V.B., Hassler, D.F., Noro, N., Furuta, M., Emmitte, K.A., Gilmer, T.M., et al. (2007). In vitro biological activity of a novel small-molecule inhibitor of polo-like kinase 1. Mol. Cancer Ther. *6*, 450–459.

Moffat, J., Grueneberg, D.A., Yang, X., Kim, S.Y., Kloepfer, A.M., Hinkle, G., Piqani, B., Eisenhaure, T.M., Luo, B., Grenier, J.K., et al. (2006). A lentiviral RNAi library for human and mouse genes applied to an arrayed viral high-content screen. Cell *124*, 1283–1298.

Müller, U., Steinhoff, U., Reis, L.F., Hemmi, S., Pavlovic, J., Zinkernagel, R.M., and Aguet, M. (1994). Functional role of type I and type II interferons in antiviral defense. Science *264*, 1918–1921.

Olsen, J.V., de Godoy, L.M., Li, G., Macek, B., Mortensen, P., Pesch, R., Makarov, A., Lange, O., Horning, S., and Mann, M. (2005). Parts per million mass accuracy on an Orbitrap mass spectrometer via lock mass injection into a C-trap. Mol. Cell. Proteomics *4*, 2010–2021.

Ong, S.E., and Mann, M. (2006). A practical recipe for stable isotope labeling by amino acids in cell culture (SILAC). Nat. Protoc. *1*, 2650–2660.

Rappsilber, J., Mann, M., and Ishihama, Y. (2007). Protocol for micro-purification, enrichment, pre-fractionation and storage of peptides for proteomics using StageTips. Nat. Protoc. *2*, 1896–1906.

Reindl, W., Yuan, J., Krämer, A., Strebhardt, K., and Berg, T. (2009). A pan-specific inhibitor of the polo-box domains of polo-like kinases arrests cancer cells in mitosis. ChemBioChem *10*, 1145–1148.

Rush, J., Moritz, A., Lee, K.A., Guo, A., Goss, V.L., Spek, E.J., Zhang, H., Zha, X.M., Polakiewicz, R.D., and Comb, M.J. (2005). Immunoaffinity profiling of tyrosine phosphorylation in cancer cells. Nat. Biotechnol. *23*, 94–101.

Shalek, A.K., Robinson, J.T., Karp, E.S., Lee, J.S., Ahn, D.R., Yoon, M.H., Sutton, A., Jorgolli, M., Gertner, R.S., Gujral, T.S., et al. (2010). Vertical silicon nanowires as a universal platform for delivering biomolecules into living cells. Proc. Natl. Acad. Sci. USA *107*, 1870–1875.

Shapira, S.D., Gat-Viks, I., Shum, B.O., Dricot, A., de Grace, M.M., Wu, L., Gupta, P.B., Hao, T., Silver, S.J., Root, D.E., et al. (2009). A physical and regulatory map of host-influenza interactions reveals pathways in H1N1 infection. Cell *139*, 1255–1267.

Steegmaier, M., Hoffmann, M., Baum, A., Lénárt, P., Petronczki, M., Krssák, M., Gürtler, U., Garin-Chesa, P., Lieb, S., Quant, J., et al. (2007). BI 2536, a potent and selective inhibitor of polo-like kinase 1, inhibits tumor growth in vivo. Curr. Biol. *17*, 316–322.

Storey, J.D., and Tibshirani, R. (2003). Statistical significance for genomewide studies. Proc. Natl. Acad. Sci. USA *100*, 9440–9445.

Tager, A.M., Kradin, R.L., LaCamera, P., Bercury, S.D., Campanella, G.S., Leary, C.P., Polosukhin, V., Zhao, L.H., Sakamoto, H., Blackwell, T.S., and Luster, A.D. (2004). Inhibition of pulmonary fibrosis by the chemokine IP-10/CXCL10. Am. J. Respir. Cell Mol. Biol. *31*, 395–404.

Villén, J., and Gygi, S.P. (2008). The SCX/IMAC enrichment approach for global phosphorylation analysis by mass spectrometry. Nat. Protoc. *3*, 1630–1638.

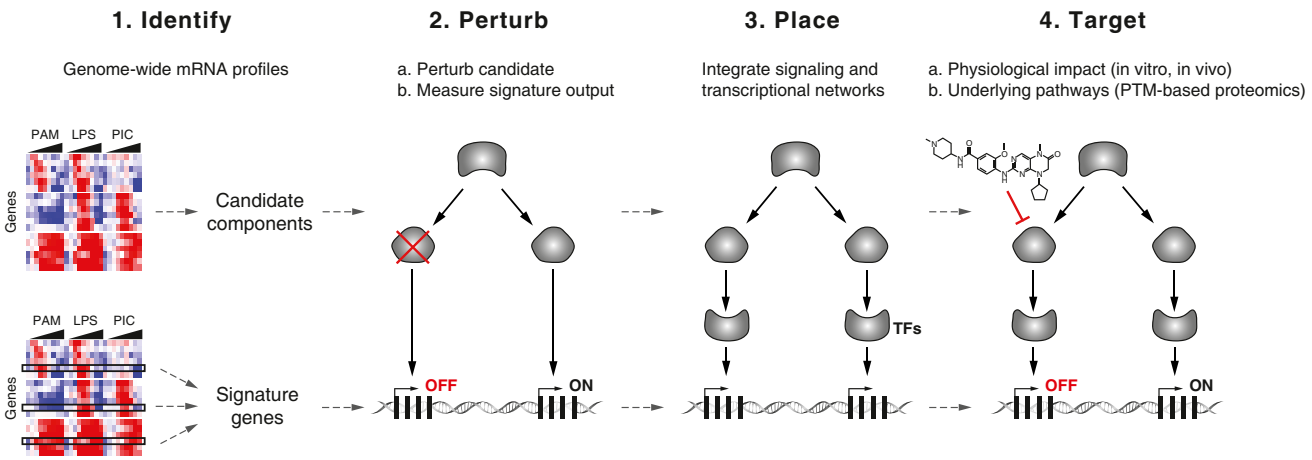

Figure S1. A Systematic Approach to Dissect Signaling Pathways, Related to Figure 1

Shown is a schematic depicting the strategy consisting of four steps (from left to right): (1) extract both candidate signaling regulators and signature genes; (2) perturb each candidate with shRNAs and measure the effect on the expression of signature genes; (3) compare perturbation profiles of signaling and transcriptional regulators to start assembling pathways; (4) use small-molecule targeting of signaling nodes of interest to (a) evaluate the physiological relevance of new signaling node and (b) identify underlying pathways by discovering downstream effector molecules.

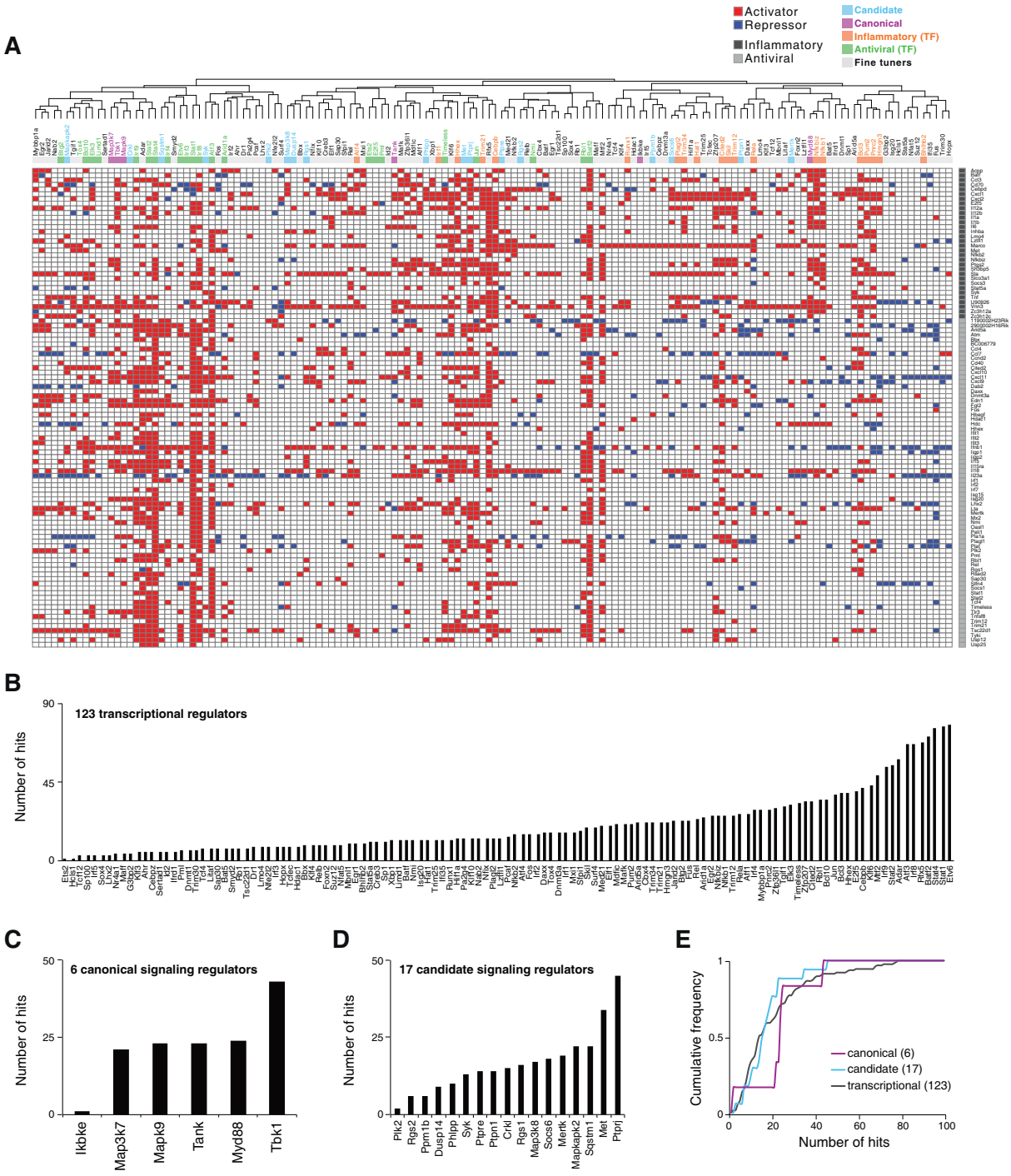

Figure S2. Perturbations of Signaling and Transcriptional Regulators Have Similar Effects on the TLR Signature Genes, Related to Figure 2

(A) Perturbation profiles of 6 canonical (purple) and 17 candidate (light blue) signaling regulators and 123 transcriptional regulators (TF) partitioned into regulators of the inflammatory (orange) and antiviral (green) programs, and fine tuners (gray), as previously defined in Amit et al. (2009). Shown are the perturbed regulators (columns) and their statistically significant effects (FDR < 2%) on each of the 118 TLR signature genes (rows). Red: significant activating relation (target gene expression decreased following perturbation); blue: significant repressing relation (target gene expression increased following perturbation); white: no significant effect. The column on the right indicates whether signature genes belong to the antiviral (light gray) or the inflammatory (dark gray) programs.

(B–D) Shown are the numbers of signature genes hits (y axis, "hits") significantly affected by knockdown of each regulator (x axis) for the regulator categories shown in A: 123 transcriptional (B) and 6 previously known (C) and 17 candidate (D) signaling regulators.

(E) Candidate signaling regulators affect a similar number of "signature" genes compared to transcriptional regulators. Shown is the cumulative distribution of the number of hits for the regulators shown in (B)–(D).

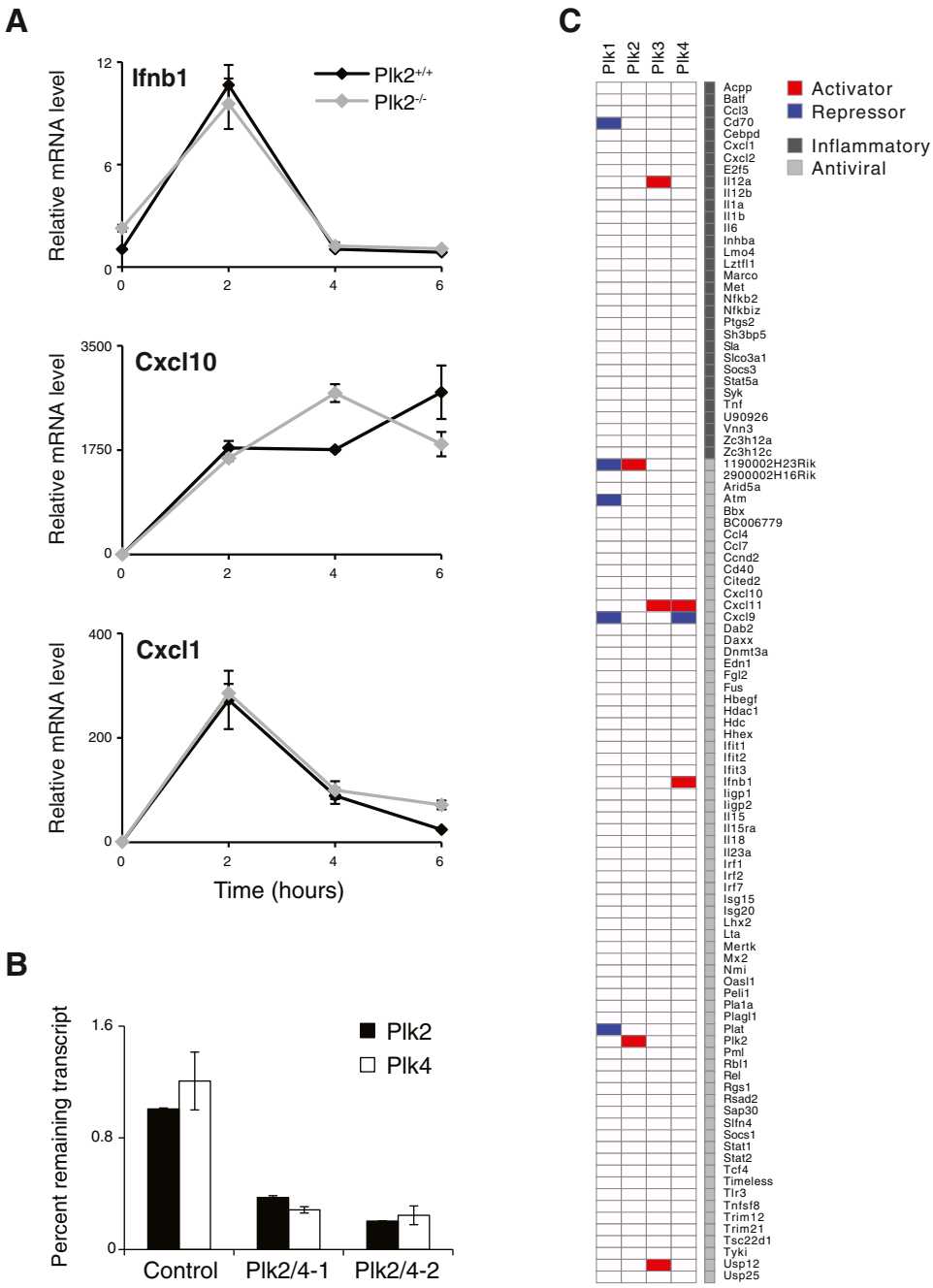

Figure S3. Individual Perturbation of Plk Family Members Does Not Affect TLR Output Gene Expression in DCs, Related to Figure 4

(A) *Plk2*-deficient BMDCs respond to LPS similarly to wild-type cells. Shown are mRNA levels (qPCR; relative to t = 0) for *Ifnb1* (left), *Cxcl10* (middle), and *Cxcl1* (right) in three replicates per time point. Error bars represent the SEM.

(B) Combinatorial knockdown levels of *Plk2* and *4* in BMDCs. Shown are mRNA levels (qPCR), relative to nontargeting shRNAs (Control), of *Plk2* and *4* in BMDCs using two independent combinations of shRNAs (*Plk2/4-1* and *-2*). Three replicates in each experiment; error bars represent the SEM.

(C) Perturbations of individual Plk family members do not affect TLR signature genes. Shown are the perturbed Plks (columns) and their statistically significant effects (FDR < 2%) on each 118 TLR signature genes (rows). Red: significant activating relation (target gene expression decreased following perturbation); blue: significant repressing relation (target gene expression increased following perturbation); white: no significant effect. The column on the right indicates whether signature genes belong to the antiviral (light gray) or the inflammatory (dark gray) programs.

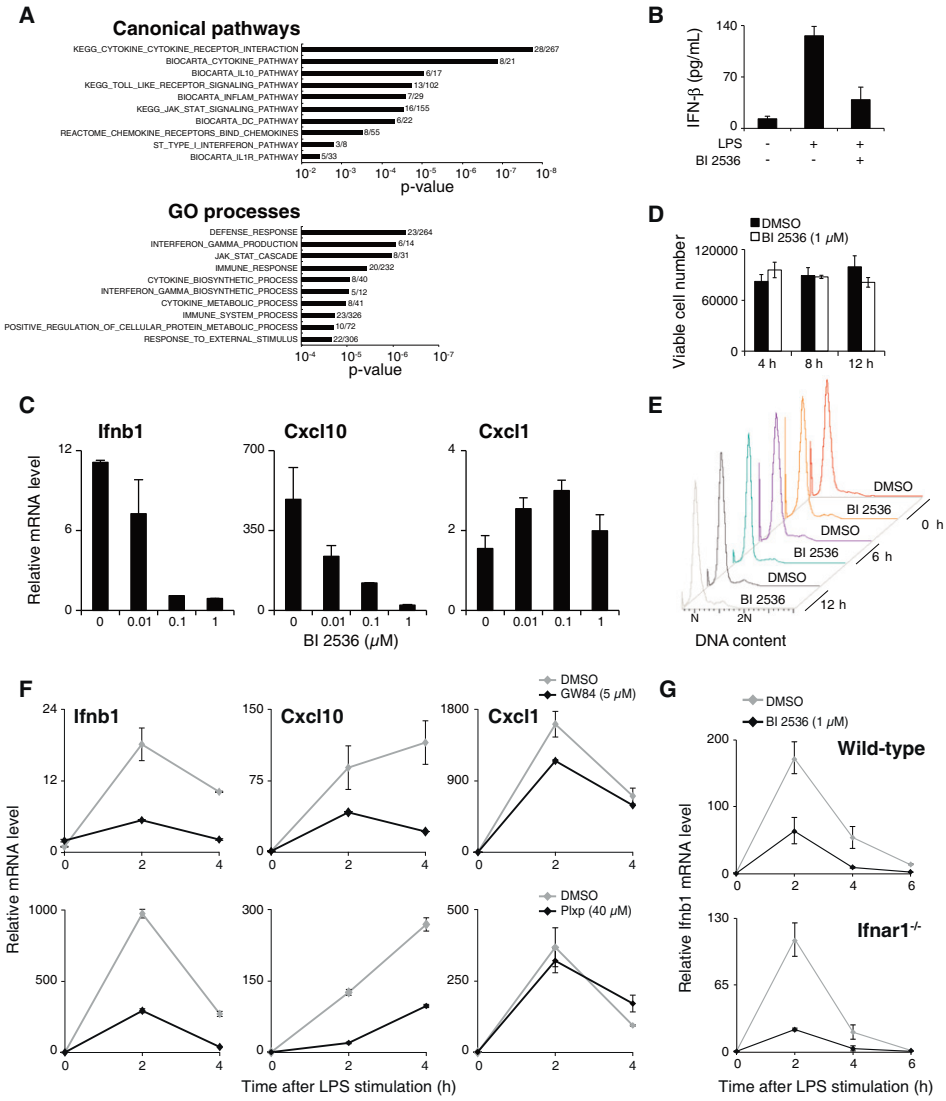

Figure S4. BI 2536-Mediated Plk Inhibition Abrogates Antiviral Cytokine Production at the Protein and mRNA Levels, without Affecting the Viability and Cell-Cycle Status of DCs, Related to Figure 4

(A) Gene enrichment analysis of BI 2536-dependent genes from microarray measurements. Overlaps between the 311 unique genes downregulated 3-fold by BI 2536 treatment upon LPS or poly(I:C) stimulation (Table S4), and Gene Ontology (GO) processes and canonical pathways (including the KEGG, REACTOME, and BIOCARTE databases present in the Molecular Signatures Database [MSigDB]; see Experimental Procedures). Shown are p values (x axis) derived from the overlaps (n/N; top of each bar) between the number of queried genes (n) and genes present in indicated genesets (N).

(B) BI 2536 strongly inhibits IFN-β secretion by BMDCs. Shown is IFN-β protein concentration (y axis; measured by ELISA) in the supernatant of BMDCs treated with DMSO vehicle (–) or BI 2536 (1 μM; +), and stimulated with LPS (+) or left unstimulated (–) for 6 hr. Three replicates in each experiment; error bars are the SEM.

(C) BI 2536 inhibits antiviral cytokine mRNA production in a dose-dependent manner. Shown are mRNA levels (y axis, qPCR; relative to vehicle control treatment) for two antiviral cytokines (*Ifnb1*, *Cxcl10*) and one inflammatory cytokine (Cxcl1) following LPS stimulation in BMDCs pretreated with increasing amounts of BI 2536 (x axis). Three replicates in each experiment; error bars are the SEM.

(D) BMDC viability is unaffected by Plk inhibition with BI 2536. Shown are viable cell numbers (y axis, measured by Alamar blue; relative to a standard curve generated using a range of cell densities) after treatment with BI 2536 (white bars) or DMSO vehicle (black bars) at different time points following addition of BI 2536 (x axis). Three replicates in each experiment; error bars are the SEM.

(E) The cell-cycle state of BMDCs remains unchanged upon Plk inhibition with BI 2536. Shown are DNA contents (flow cytometry) of BMDCs stained with propidium iodide (PI) after treatment with BI 2536 or DMSO vehicle control for 0, 6, and 12 hr.

(F) Plk inhibitors structurally unrelated to BI 2536 also abrogate transcription of mRNAs for antiviral cytokines following stimulation with LPS. Shown are mRNA levels (qPCR; relative to t = 0) for *Ifnb1*, *Cxcl10*, and *Cxcl1* in BMDCs stimulated with LPS and treated with GW843682X (GW84; top) or Poloxipan (Plxp; bottom) (black line), or with DMSO vehicle (gray line) for 1 hr prior to stimulation. Three replicates for each experiment; error bars are the SEM.

(G) Plks are directly downstream of TLR engagement. Shown are Ifnb1 mRNA levels (y axis, qPCR; relative to t = 0) following LPS stimulation for indicated times (x axis) in wild-type (top) and *Ifnar1*$^{-/-}$ (bottom) BMDCs treated with BI 2536 (1 μM; black) or vehicle control (DMSO; gray). Error bars represent the SEM.

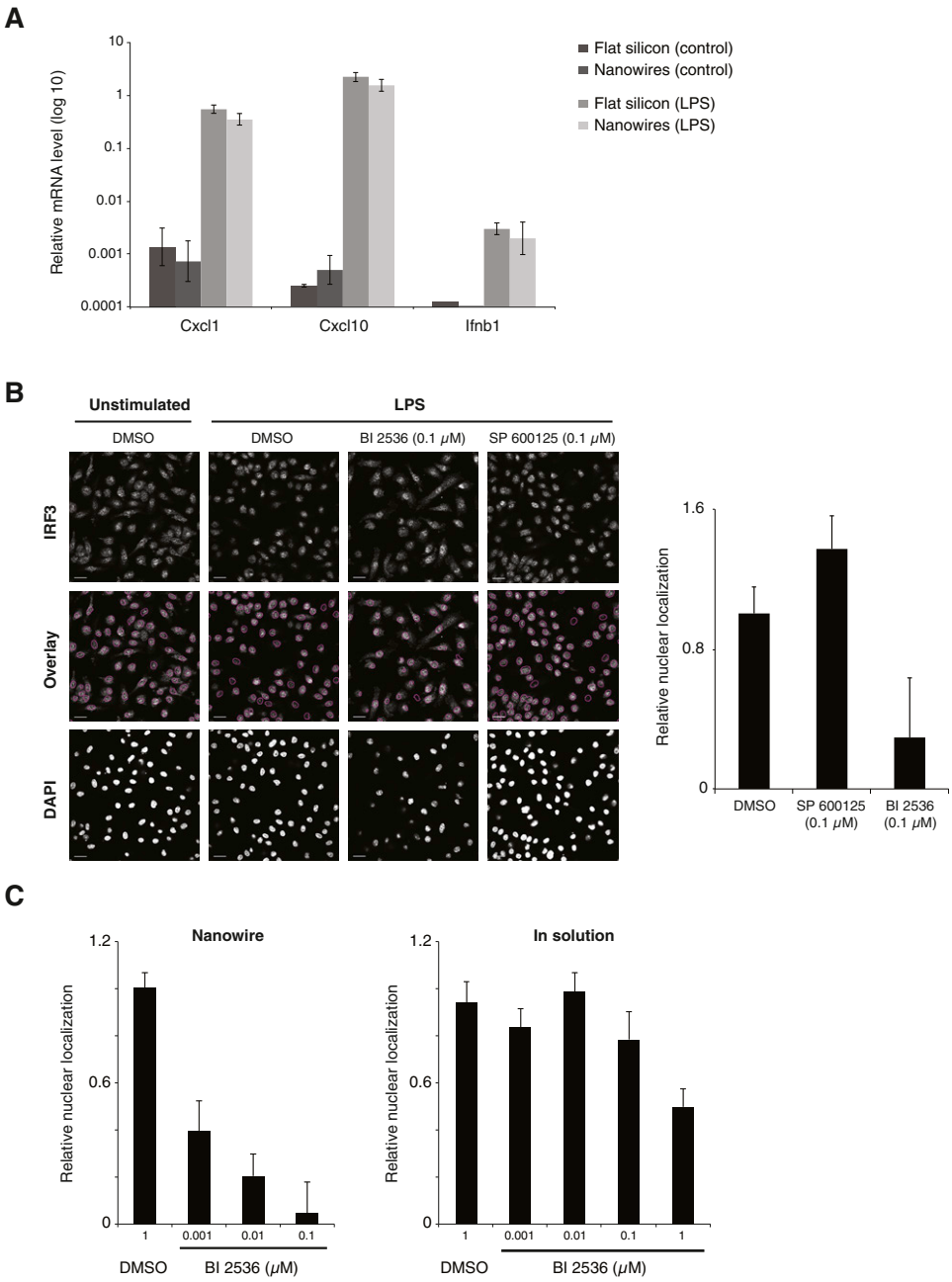

Figure S5. BI 2536-Mediated Plk Inhibition Blocks IRF3 Nuclear Translocation in LPS-Stimulated DCs, Related to Figure 5

(A) DCs plated on vertical silicon NW respond normally to TLR stimulation. Shown are cytokine mRNA levels (qPCR; relative to Gapdh mRNA) in BMDCs plated on NW or a flat silicon surface, and stimulated (LPS) or left untreated (control). Left to right: *Cxcl1*, *Cxcl10*, *Ifnb1*. Three replicates in each experiment; error bars are the SEM.

(B) BI 2536 inhibits IRF3 nuclear translocation following LPS stimulation. Shown are confocal micrographs (left panel) of BMDCs plated on vertical silicon NW precoated with vehicle control (DMSO), Plk inhibitor (BI 2536), or control Jnk inhibitor (SP 600125) and stimulated with LPS for 45 min (reflecting peak time of nuclear translocation for IRF3 in the context of LPS stimulation) or left unstimulated. Cells were analyzed for DAPI and IRF3 staining. Scale bars, 5 μM. Nuclear translocation (from confocal micrographs) of IRF3 was quantified (right panel) using DAPI staining as a nuclear mask (purple circles on micrographs) to determine the ratio of total versus nuclear fluorescence (y axis) in BMDCs cultured on NW coated with BI 2536, SP 600125, or vehicle control (DMSO; x axis). Three replicates in each experiment; error bars are the SEM.

(C) Decrease in IRF3 nuclear translocation may be more efficient with NW-mediated delivery of BI 2536 than with delivery in solution. Shown are quantifications of confocal micrographs from BMDCs plated on vertical NW precoated with different amounts of BI 2536 (Nanowire; left panel) or left blank to allow in-solution delivery of BI 2536 (In solution; right panel). Cells were stimulated with poly(I:C) for 2 hr prior to staining for DAPI and IRF3 as in (B). Error bars represent the SEM.

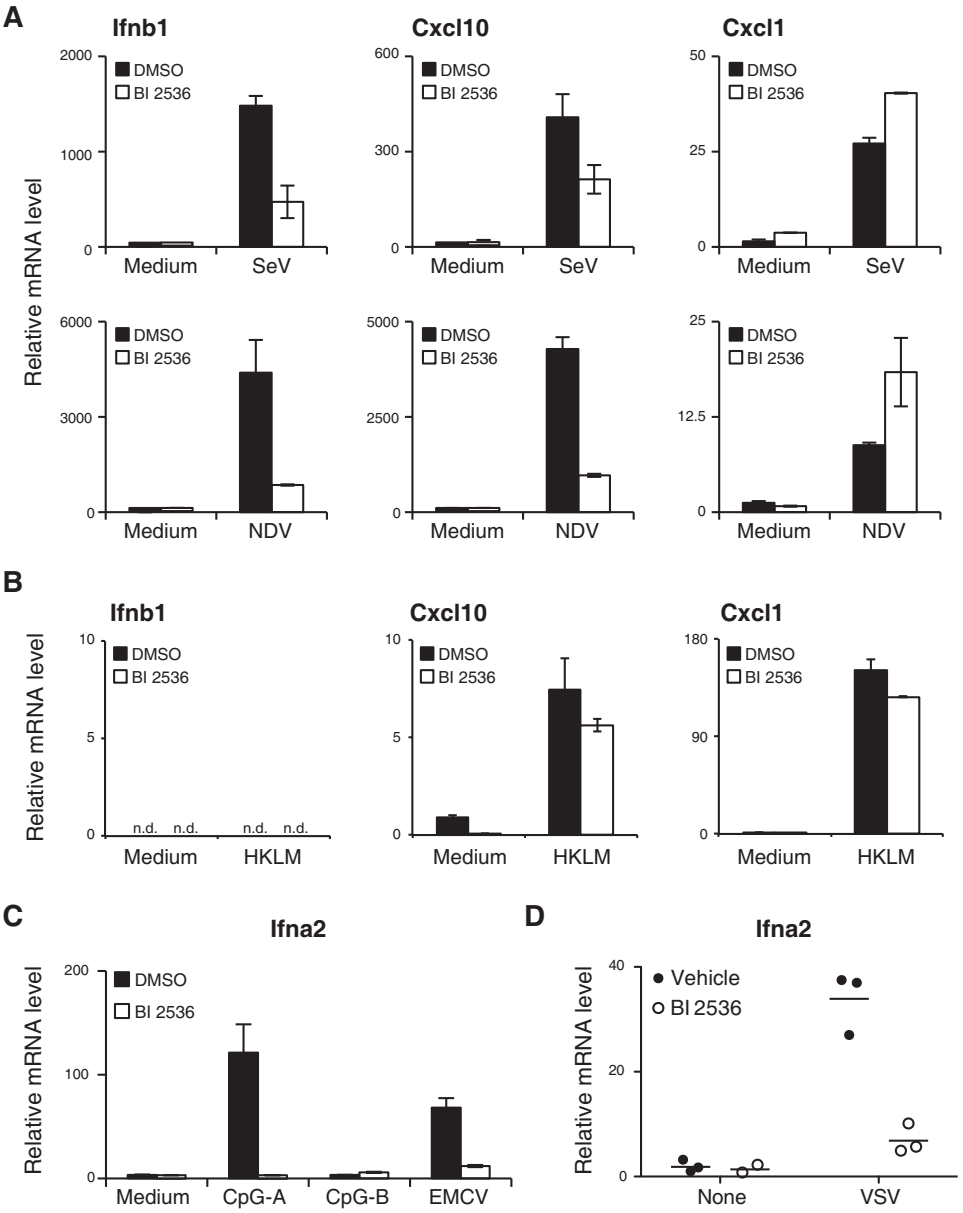

Figure S6. Plks Are Critical in Antiviral Responses In Vitro and In Vivo, Related to Figure 6

(A) Plks are critical in RIG-I-mediated antiviral responses in vitro in DCs. Shown are mRNA levels (qPCR; relative to control, "medium") in conventional DCs (GM-CSF-induced BMDCs) treated with BI 2536 (white bars) or DMSO vehicle (black bars) and infected at a multiplicity of infection (moi) 1 with Sendai virus (SeV; top) or Newcastle disease virus (NDV; bottom). Three replicates in each experiments; error bars are the SEM.

(B) Plk inhibition does not affect DC response to *Listeria monocytogenes*, a natural TLR2 agonist. Shown are mRNA levels (qPCR; relative to t = 0) for *Ifnb1*, *Cxcl10*, *and Cxcl1* in BMDCs stimulated with heat-killed *Listeria monocytogenes* (HKLM; moi 5) and treated with BI 2536 (white bars) or with DMSO vehicle (black bars) for 1 hr prior to stimulation. Three replicates for each experiment; error bars are the SEM.

(C) Plks are critical in type I interferon $\alpha 2$ (*Ifna2*) gene production by pDCs. Shown is the mRNA level (qPCR; relative to control, "medium") of *Ifna2* in pDCs (Flt3L-induced BMDCs) treated with BI 2536 (1 μM; white bars) or DMSO control (black bars) and stimulated with CpG-A or -B or infected with EMCV (moi 10). Three replicates in each experiment; error bars are the SEM.

(D) Plk inhibition in vivo inhibits type I IFN $\alpha 2$ production in the lymph node. Shown is *Ifna2* mRNA level (qPCR; relative to uninfected animals) from popliteal lymph nodes of mice injected with BI 2536 (white circles) or DMSO vehicle (black circles) prior to and during the course of infection with VSV intra-footpad. Nodes were harvested 6 hr post-infection. Each circle represents one animal (n = 3). Data are representative of two or three independent experiments for each condition.

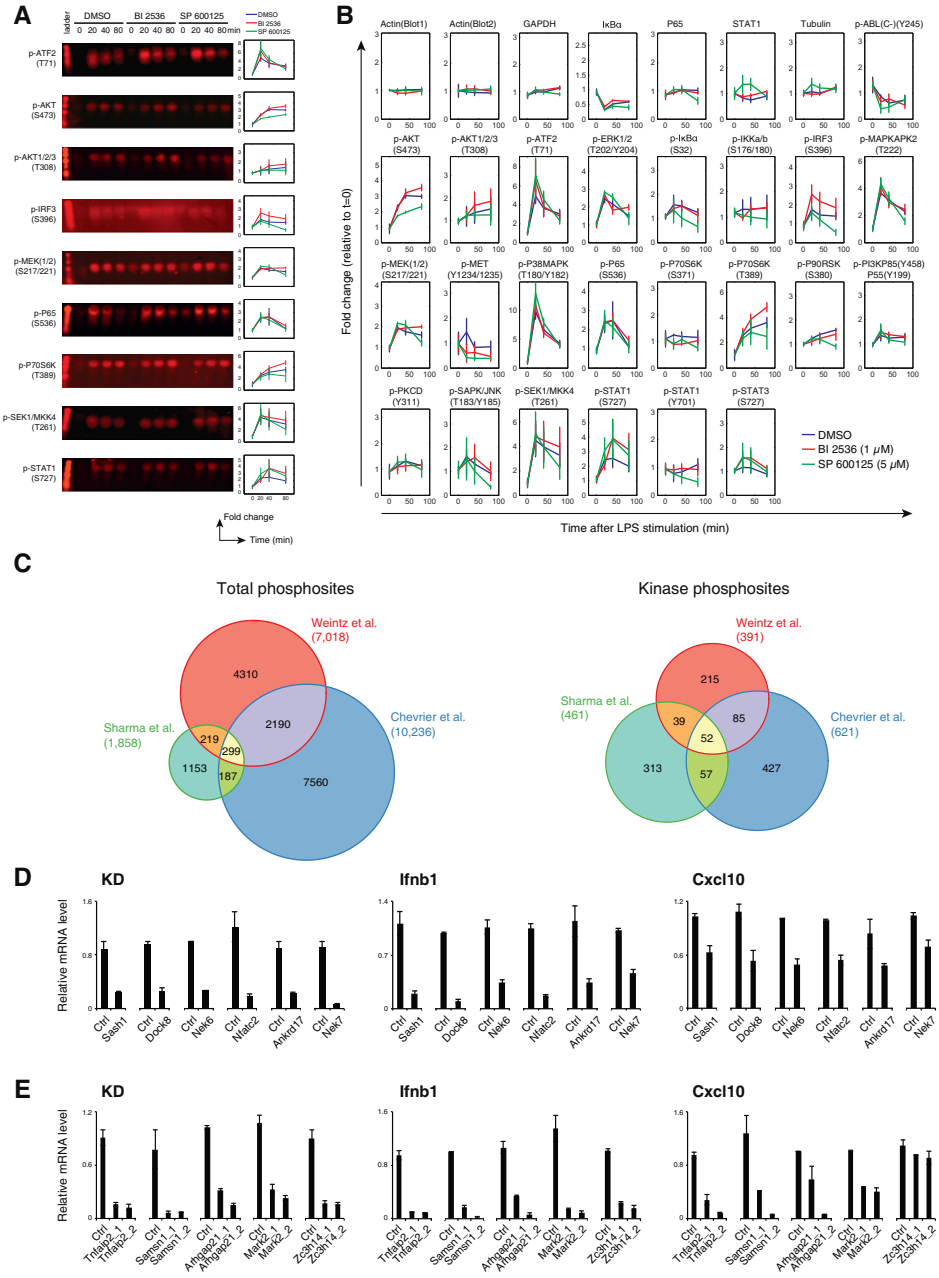

Figure S7. Plk Inhibition Does Not Affect Known TLR Signaling Components but Affects Eleven Newly Identified Plk-Dependent Phosphoproteins, Related to Figure 7

(A and B) BI 2536-mediated Plk inhibition does not affect protein and/or phosphorylation levels of known TLR signaling nodes. (A) Shown are representative MWA (see Experimental Procedures) blots obtained from analyzing lysates from BMDCs pretreated with DMSO, BI 2536 (1 μM), or SP 600125 (5 μM) and stimulated with LPS for 0, 20, 40, 80 min. Blots were analyzed using indicated antibodies (leftmost), and fold change in fluorescence signals was quantified relative to t = 0 (right; see Experimental Procedures). Error bars are the SEM of triplicate MWA blots. (B) Shown are the differential protein and phosphorylation levels (fold change; y axis) of 6 proteins and 23 phosphosites in BMDCs treated with BI 2536 (red line), control JNK inhibitor (SP 600125; green line), or DMSO vehicle (blue line), and stimulated with LPS (0, 20, 40, 80 min; x axis). Band intensities on MWA blots were quantified using Li-Cor Odyssey analysis software (Experimental Procedures). For each antibody, data were normalized to β-actin levels; error bars are the SEM of triplicate MWA blots.

(C and D) Eleven Plk-dependent phosphoproteins are critical for TLR-mediated antiviral responses in DCs. Shown are mRNA levels (qPCR; relative to non-targeting control shRNAs, Ctrl) for knockdown (KD) efficiency (left), *Ifnb1* (middle), and *Cxcl10* (right) in BMDCs following LPS stimulation. Genes with one and two shRNAs are shown in (C) and (D), respectively. Three replicates in each experiment; error bars are the SEM.

(E) Comparison of phosphosites identified in our study and in two recent reports (Weintz et al., 2010 and Sharma et al.. 2010). Shown are proportional Venn diagrams of the total unique phosphosites identified by the 3 studies (left), and the phosphosites harbored by kinases only (right). Total numbers of unique phosphosites per study are indicated in parentheses. Error bars are the SEM.